

Magnetic Fields in the Relativistic Jets of Active Galactic Nuclei

Denise C. Gabuzda

Physics Department, University College Cork, Cork, Ireland
email: d.gabuzda@ucc.ie

Abstract. An abundance of information about the magnetic (\mathbf{B}) fields of relativistic AGN jets has been obtained through radio polarization observations made on a wide range of scales, from the parsec scales probed by Very Long Baseline Interferometry to the kiloparsec scales probed by instruments such as the the Jansky Very Large Array and e-MERLIN. The observed radio emission is synchrotron radiation, for which the linear polarization angles in optically thin regions is orthogonal to the local synchrotron \mathbf{B} fields. The characteristic \mathbf{B} field structures observed for these jets on parsec scales are described. A key question is whether \mathbf{B} field structures observed in particular AGN jets come about primarily due to “global” effects such as the intrinsic \mathbf{B} field of the jet itself, which is expected to be helical, or local phenomena such as shocks, shear and bending of the jets. Observational criteria that can be used to try to distinguish between various possible origins for observed \mathbf{B} field structures are described. There is now considerable evidence that the relativistic jets of AGNs do indeed carry helical \mathbf{B} fields, with the observed polarization also sometimes appreciably influenced by local effects. Patterns seen in the helical \mathbf{B} field components, indicated for example by Faraday rotation observations, provide unique information about the processes involved in the generation of these helical \mathbf{B} fields. The collected observations on parsec and kiloparsec scales provide weighty evidence that an important role is played by the action of a cosmic “battery” that acts to generate an inward current along the jet axis and an outward current in a more extended region surrounding the jet.

Keywords.

1. AGN Jets and Helical/Toroidal \mathbf{B} fields

Core-dominated AGN almost universally display one-sided core-jet structures on VLBI scales, consistent with a picture in which the jets ejected from the active nucleus are highly relativistic and we are detecting only the Doppler-boosted approaching jet (e.g. [Lister & Homan 2005](#)). Apparent superluminal motions are also extremely common, again consistent with relativistic jets oriented at relatively small angles to the line of sight ([Kellermann *et al.* 2004](#)).

It has long been believed theoretically that the mechanism launching the jets from the vicinity of the central engine is electromagnetic in nature. The main mechanisms considered are those proposed by [Blandford & Znajek \(1977\)](#), where the jets are launched from the immediate vicinity of the central black hole, and by [Blandford & Payne \(1982\)](#), where the jets are launched from the surrounding accretion disk. Numerical simulations have demonstrated the generation of helical magnetic (\mathbf{B}) fields associated with the jets, due to the “winding up” of an initial longitudinal field component (e.g., [Barniol Duran *et al.* 2017](#)). This leads to the clear expectation on theoretical grounds that AGN jets should carry helical \mathbf{B} fields, which should have certain observational consequences. These fields may effectively be manifest as toroidal fields when the azimuthal component of the field is very dominant. Observational evidence for the presence of helical jet \mathbf{B} fields provides direct support for this widely accepted theoretical picture.

The highly relativistic jets of AGN are also typically extremely narrow, obviously well collimated structures, with the jets sometimes remaining collimated all the way out to kiloparsec scales. One natural way for this to come about is self-collimation by the azimuthal component of the helical \mathbf{B} field that is generated when the jets are launched.

A key physical phenomenon in relation to the observational detection of the presence of helical jet \mathbf{B} fields is Faraday rotation: a rotation of the plane of polarization of an electromagnetic wave as it passes through a region with free charges and magnetic field (i.e., a magnetized plasma). This rotation of the linear polarization angle comes about due to the different indices of refraction of the right circularly polarized (RCP) and left circularly polarized (LCP) components of the polarized wave, leading to different speeds of propagation through the magnetized medium. This difference in the speeds of the RCP and LCP components induces a delay between them, manifest as a rotation in the plane of linear polarization. The amount of rotation depends on the strength of the ambient magnetic field \mathbf{B}_{amb} , the number density of free electrons in the Faraday-rotating plasma n_e , the electron charge e and mass m , and the wavelength of the radiation λ :

$$\chi = \chi_o + RM\lambda^2 \quad RM = \frac{e^3}{8\pi^2\epsilon_o m_e^2 c^3} \int n_e \mathbf{B}_{amb} \cdot d\mathbf{l} \quad (1.1)$$

where χ is the observed polarization angle, χ_o the intrinsic emitted polarization angle, ϵ_o the permittivity of free space, and c the speed of light; the integral is carried out over the line of sight from the source to the observer.

The magnitude of the Faraday rotation measure RM depends on both n_e and the line-of-sight component of \mathbf{B}_{amb} , while the sign of the Faraday rotation is determined purely by the direction of the line-of-sight component of \mathbf{B}_{amb} (toward or away from the observer). The action of Faraday rotation can be identified through the λ^2 dependence of the observed polarization angle χ .

As was pointed out by Blandford (1993), if a jet has a helical \mathbf{B} field, this should give rise to a Faraday-rotation gradient across the jet, due to the systematically changing line-of-sight component of the \mathbf{B} field across the jet. Thus, the detection of transverse Faraday-rotation gradients across AGN jets can provide a powerful diagnostic for the presence of an azimuthal field component that may be associated with a helical jet \mathbf{B} field. Furthermore, the presence of such an azimuthal field component straightforwardly implies the presence of a current in the jet, whose direction is given by the usual right-hand rule from university physics. Figure 1 shows an example of an AGN jet with a clear, statistically significant transverse RM gradient across its jet, with the direction of the associated azimuthal \mathbf{B} field component shown together with the inferred direction of the jet current. Statistically significant transverse RM gradients, interpreted as reflecting the presence of an azimuthal \mathbf{B} -field component, have now been detected across about 50 AGN jets on parsec scales (Gabuzda *et al.* 2018) and roughly a dozen AGN jets on larger scales of tens to thousands of parsecs (Christodoulou *et al.* 2016, Knuettel *et al.* 2017). This provides direct evidence for toroidal or helical \mathbf{B} fields in AGN jets on all scales accessible to direct imaging in the radio.

The presence of helical jet \mathbf{B} fields will also give rise to certain characteristic polarization (\mathbf{B} -field) structures in AGN jets, as is discussed in the following section. Other recent observations that have been interpreted as manifestations of helical jet \mathbf{B} fields include an increase (rather than the expected decrease) in degree of polarization with increasing wavelength (so-called “inverse depolarization”, Homan 2011), variability of jet ridge lines (Cohen *et al.* 2015), variability of the Faraday rotation sign (Lico *et al.* 2017), double polarization angle rotations (Cohen 2017), and circular polarization (Gabuzda 2015). This suggests that helical \mathbf{B} fields carried by AGN jets may provide a framework for understanding a wide range of their properties and the behaviours they display.

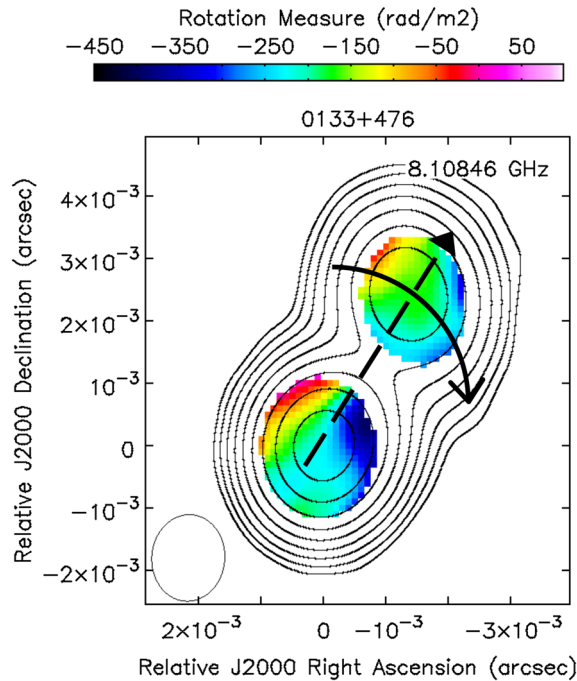


Figure 1. Relationship between an observed transverse RM gradient, the direction of the associated azimuthal \mathbf{B} field component (solid curved arrow), and the inferred direction of the current (dashed arrow). RM image adapted from Gabuzda (2018).

2. B Field Structures of AGN Jets: Global or Local Origin?

It has been noted since the earliest VLBI polarization images were analyzed that the observed polarization in the jets of AGN on parsec scales tends to lie either parallel to or perpendicular to the local jet direction, with the inferred direction of the associated jet \mathbf{B} field being orthogonal to the direction of the polarization. Commonly observed polarization patterns correspond to (a) extended regions of longitudinal \mathbf{B} field, (b) regions of orthogonal \mathbf{B} field associated with bright, compact regions, (c) extended regions of orthogonal \mathbf{B} field, (d) spine-sheath transverse \mathbf{B} -field structure, (e) longitudinal \mathbf{B} field offset toward one side of the jet, and (f) longitudinal \mathbf{B} field around a bend in the jet; here, “longitudinal” and “orthogonal” are relative to the direction of the jet (see the schematic of these polarization configurations shown by Gabuzda (2015)). This should come about naturally if the jets locally exhibit approximately cylindrical symmetry: the \mathbf{B} field can then always be separated into longitudinal and orthogonal components projected onto the sky (e.g. Lyutikov *et al.* 2005).

Thus, the jets are expected theoretically to carry helical \mathbf{B} fields, and direct observational evidence for such fields has been found through the detection of statistically significant transverse Faraday-rotation gradients across AGN jets on scales from parsecs to kiloparsecs. This makes it natural to consider which of these commonly observed \mathbf{B} -field patterns could be associated with these helical \mathbf{B} fields.

2.1. Structures associated with helical fields

Helical jet \mathbf{B} fields could give rise to many of the characteristic polarization patterns referred to above.

- Extended regions of longitudinal or orthogonal \mathbf{B} field could be associated with helical jet \mathbf{B} fields with comparatively low and high pitch angles (i.e., comparatively “loosely wound” or “tightly wound” helical fields), respectively.
- Spine–sheath transverse polarization structure implying orthogonal \mathbf{B} fields near the center of the jet and longitudinal \mathbf{B} fields at one or both edges of the jet could be associated with a helical field, with the azimuthal component of the field dominant near the center of the jet and the longitudinal component dominant near the jet edges, projected onto the sky (e.g., Pushkarev *et al.* 2005, Lyutikov *et al.* 2005). In this case, this should also give rise to an increase in the degree of polarization toward the jet edges.
- Some combinations of pitch angle and viewing angle give rise to projected helical \mathbf{B} -field configurations with longitudinal field on one side of the jet and transverse field on the other, which may also be observed as longitudinal field offset toward one side of the jet if the transverse field has much weaker polarization (e.g. Murphy *et al.* 2013).

2.2. Structures due to local effects

The main local effects that have been suggested as possible origins of observed polarization features are shear with the surrounding medium acting to stretch out the magnetic field along the flow, and transverse shocks, which amplify the \mathbf{B} field component in the plane of compression. Other factors that are increasingly believed to play significant roles include turbulence and magnetic reconnection.

Shear will enhance the longitudinal field component, and has been proposed as an explanation for regions of longitudinal \mathbf{B} field in AGN jets, especially at the jet edges. Note, however, that such regions could also come about due to the presence of helical jet \mathbf{B} fields. Shocks enhance the local orthogonal field component; compact features with orthogonal \mathbf{B} field are good candidates for localized regions of transverse shocks, although extended regions of extended orthogonal field are probably more plausibly explained by the presence of a relatively high-pitch-angle helical field.

Turbulence is almost certainly present in AGN jets to some degree, and could be induced by mechanisms such as Kelvin–Helmholtz instability or current-driven (kink) instability in helical or toroidal jet \mathbf{B} fields (e.g. Singh *et al.* 2016, Striani *et al.* 2016, de Gouveia Dal Pino *et al.* these proceedings). Turbulence could, in turn, lead to magnetic reconnection. It is likely that both of these effects play important roles, particularly in relation to variability, particle acceleration and very high energy emission (e.g., de Gouveia Dal Pino *et al.* these proceedings). Magnetic reconnection suggests the presence of magnetic field reversals, but it is not entirely clear how these can be detected in polarization images. The general impact of these effects should be to partially destroy the overall polarization patterns due to coherent helical or toroidal fields. It may be that turbulence acts primarily to reduce the degree of polarization, leaving the overall polarization patterns more or less intact, whereas magnetic reconnection would likely bring about appreciable changes in the initial field configuration. Regions that display variability and unusual \mathbf{B} -field structures may be good candidates for regions of magnetic reconnection.

Another less discussed mechanism that can also potentially play a role is enhancement of the local longitudinal \mathbf{B} field at the outer edges of bends in the jet, sometimes called “curvature induced polarization”. This could either amplify an existing longitudinal field component, for example, associated with a helical jet \mathbf{B} field, or induce a net longitudinal component in an initially tangled field, analogous to the ability of a shock to induce a net orthogonal component in an initially tangled field.

It is clear that helical jet \mathbf{B} fields can potentially provide a natural explanation for essentially all of the observed characteristic \mathbf{B} -field patterns observed in AGN jets.

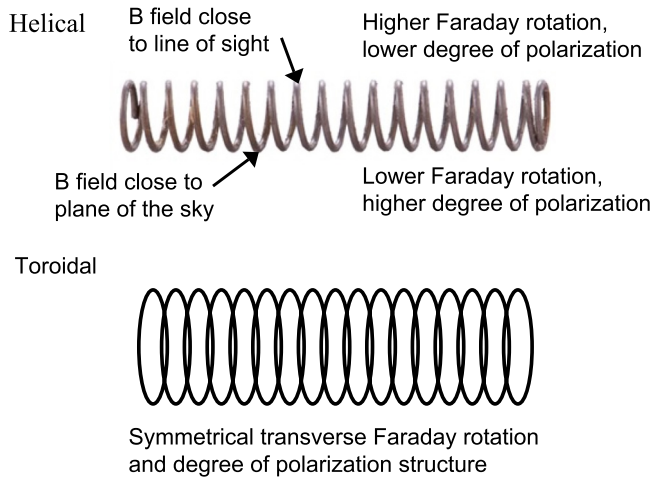


Figure 2. Schematic illustrating differences in polarization asymmetry for jets carrying helical versus toroidal \mathbf{B} fields.

However, it is also the case that the origin of a given \mathbf{B} -field structure may not be obvious from the observed polarization-angle distribution alone, and additional information is usually required as a basis for sound interpretation, such as the distribution of the degree of polarization, information about Faraday rotation and Faraday-rotation gradients occurring in the vicinity of the jet etc. Of course, in general, we might expect situations where there is a contribution from both the intrinsic helical \mathbf{B} field of the jet itself and local phenomena such as shocks and shear.

2.3. Helical versus toroidal fields

An important question is whether the azimuthal field component revealed by a transverse RM gradient is associated with a helical or a toroidal \mathbf{B} field. In general, it is only asymmetry of the intensity and polarization profiles across the jet that can distinguish observationally between a helical field (with an ordered longitudinal component) and a toroidal field (without a net longitudinal component, because this component is either absent or disordered). The key point here is that the synchrotron intensity and degree of polarization are determined by the component of the jet \mathbf{B} field in the plane of the sky (e.g., a \mathbf{B} field directed precisely toward the observer would give no linear polarization).

Figure 2 shows a schematic visually illustrating why a helical field generally gives rise to asymmetric intensity and linear polarization profiles across the jet, while a toroidal field gives rise to symmetric profiles. This figure shows helical and toroidal fields viewed side-on. The toroidal field should give rise to symmetric intensity and polarization profiles, independent of viewing angle. However, due to the presence of a longitudinal component in the helical field, the overall field usually lies predominantly along the line of sight along one edge of the jet, where it gives rise to lower degrees of polarization, and predominantly in the plane of the sky at the other edge of the jet, where it gives rise to higher degrees of polarization. Only for particular viewing angles and helical pitch angles will a helical \mathbf{B} field give rise to symmetrical intensity and polarization structures (see, e.g., [Murphy et al. 2013](#)).

In addition, the fact that Faraday rotation is proportional to the line-of-sight component of the ambient magnetic field provides additional potential tests of consistency of observations with the presence of helical \mathbf{B} fields in jets displaying transverse Faraday RM gradients. The picture depicted in Fig. 2 predicts that the side of such a jet with the

higher degree of polarization (dominant \mathbf{B} -field component in the plane of the sky) should display a lower amount of Faraday rotation, whereas the side of the jet with the lower degree of polarization should display a higher amount of Faraday rotation. Indeed, some cases where this pattern is observed have been noted (Murphy *et al.* 2013, Gabuzda *et al.* 2018).

3. Overall Patterns in the \mathbf{B} Fields/Axial Currents of AGN Jets

As was noted in the first section of this article, the direction of an observed transverse Faraday RM gradient across an AGN jet implies a direction for the azimuthal field component giving rise to the gradient, which, in turn, implies the direction for a current associated with this toroidal field (Fig. 1). The direction of the azimuthal component of the jet's helical field is essentially determined by the direction of the rotation of the central black hole and accretion disk, together with the direction of the longitudinal component of the initial field that is "wound up" by the rotation.

In this simplest picture, we would expect to see a particular direction for the observed transverse RM gradient all along the jet. However, in fact, reversals in the directions of observed transverse RM gradients, either with distance along the jet or with time, have been observed for a number of AGN jets (Gabuzda *et al.* 2018 and references therein). A recently discovered example of such an RM-gradient reversal is shown in Fig. 3. This can be understood in a picture with a nested helical-field structure, with the directions of the azimuthal field components being opposite in the inner and outer regions of helical field (Mahmud *et al.* 2013). In this case, a change in the direction of the net observed RM gradient could be due to a change in which region of helical field (inner or outer) makes the dominant contribution to the overall Faraday rotation.

Such a nested helical-field configuration is predicted by the "cosmic battery" model described by Contopoulos *et al.* (2009) and Christodoulou *et al.* (2016). Further, this model predicts that the orientations of the azimuthal components of the inner and outer regions of helical field are not random: the inner region of helical field should have a counterclockwise azimuthal component projected on the plane of the sky, associated with an inward current along the jet axis, while the outer helical field should have a clockwise azimuthal component projected onto the sky, associated with a more extended region of outward current (essentially present between the two regions of helical field).

Sufficient statistics to test this picture have recently become available. Gabuzda *et al.* (2018) have demonstrated that the collected data on transverse RM gradients detected across about 50 parsec-scale AGN jets indicate a statistically significant predominance of *inward* currents (probability of the predominance being spurious $\simeq 0.40\%$). In contrast, the results of Christodoulou *et al.* (2016), supplemented by the more recent results of Knuettel *et al.* (2017), indicate a highly statistically significant predominance of *outward* currents on decaparsec–kiloparsec scales (probability of the predominance being spurious $\simeq 0.05\%$). These observations are consistent with a picture in which the jets have a nested helical-field configuration, with current loops oriented roughly orthogonal to the accretion disk, with the current flowing inward along the jet axis, away from the axis in the accretion disk, outward in an extended region around the jet, and back toward the jet axis in a region near the termination of the jet. This is broadly similar to the set of currents and \mathbf{B} fields in a co-axial cable, but on a grand scale.

4. Summary

AGN jets are expected theoretically to carry helical \mathbf{B} fields, due to the joint action of the rotation of the central black hole and accretion disk and the jet outflow. In fact, there is now substantial observational evidence that many or all jets do carry helical

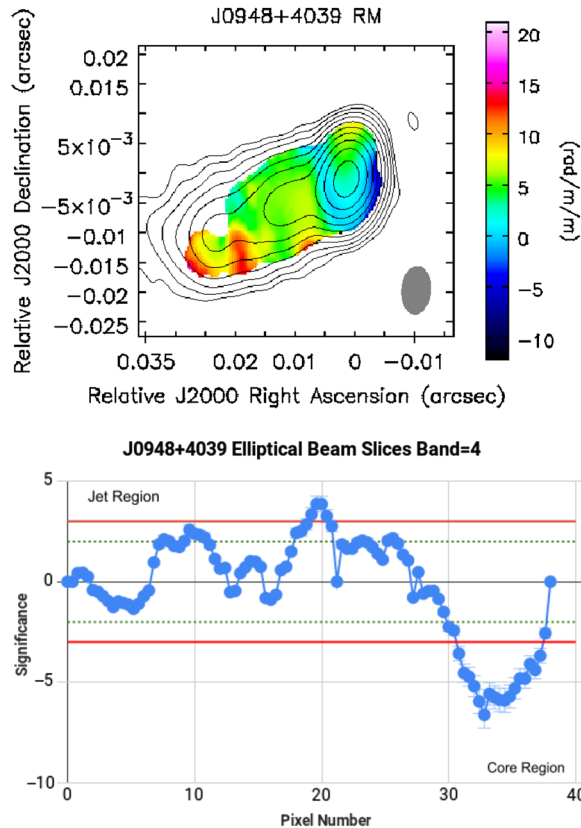


Figure 3. Transverse RM gradients across the VLBI jet of J0948+4039. The top panel shows the Faraday rotation map made using VLBA data obtained at 1.8+1.4+2.2+5.0 GHz, with maximum RM uncertainties of 3 rad/m². Oppositely directed transverse RM gradients can be seen in the core region and jet. The lower panel shows the significances of a series of RM slices taken perpendicular to the jet. The gradients in the core region have significances exceeding 5 σ , and there are fairly extended regions in the jet with transverse RM gradients with significances of 2–4 σ . The dotted green and solid red horizontal lines show significances of 2 σ and 3 σ , respectively.

B fields, most importantly, the detection of statistically significant transverse Faraday RM gradients across some 50 AGN jets on parsec scales, as well as about a dozen AGN jets on larger scales of tens to thousands of parsec. This realization is now leading to a variety of interpretations of observed properties and behaviour exhibited by AGN jets in the framework of models with helical jet **B** fields.

Furthermore, many of the characteristic polarization/magnetic-field structures observed in AGN jets on parsec scales can be understood as manifestations of a helical jet **B** field. At the same time, some are also consistent with the action of local agents, such as shocks, shear, and jet bending. It can be difficult to unambiguously identify the origin of observed polarization structures in particular jets in practice without incorporating additional information about the distribution of the degree of polarization, the morphology of the jet, the distribution of Faraday rotation in the vicinity of the jet, and the possible presence of transverse RM gradients across the jet. In many cases, it is likely that the observed polarization structure is produced by both the intrinsic helical **B** field of the jet and the action of various local factors.

The direction of a transverse RM gradient across an AGN jet implies a direction for the azimuthal \mathbf{B} -field component producing it, which, in turn, implies the direction for the net current flowing inside the region occupied by this toroidal field. The collected data on transverse RM gradients observed on parsec to kiloparsec scales demonstrate a statistically significant predominance of inward currents along the jet axis on parsec scales, and of outward currents on decaparsec–kiloparsec scales, presumably in a more extended region surrounding the jet. This is fully consistent with the “cosmic battery” model described by Contopoulos *et al.* (2009) and Christodoulou *et al.* (2016). In this picture, the systems of currents and fields in AGN jets and their accretion disks are essentially similar to those for giant co-axial cables.

References

- Barniol Duran, R., Tchekhovskoy, A. & Giannios, D. 2017, *MNRAS*, 469, 4957
- Blandford, R. D. 1993, in *Astrophysical Jets* (Cambridge University Press), p. 26
- Blandford, R. D. & Payne, D. G. 1982, *MNRAS*, 199, 883
- Blandford, R. D. & Znajek, R. L. 1977, *MNRAS*, 179, 433
- Christodoulou, D., Gabuzda, D., Knuettel, S., Contopoulos, I., Kazanas, D. & Coughlan, C. 2016, *A&A*, 591, A61
- Cohen, M. H. 2017, *Galaxies*, 5, 12
- Cohen, M. H., Meier, D. L., ARshakian, T. G., Clausen-Brown, E., Homan, D. C., Hovatta, T., Kovalev, Y. Y., Lister, M. L., Pushkarev, A. B., Richards, J. L. & Savolainen, T. 2015, *ApJ*, 803, 3
- Contopoulos, I., Christodoulou, D., Kazanas, D. & Gabuzda, D. C. 2009, *ApJ*, 702, L148
- Gabuzda, D. C. 2015, in *The Formation and Disruption of Black Hole Jets, Astrophysics and Space Science Library*, 414, p. 117
- Gabuzda, D. C. 2018, *Galaxies*, 6, 9
- Gabuzda, D. C., Nagle, M. & Roche, N. 2018, *A&A*, 612, A67
- Homan, D. C. 2011, *ApJ*, 757, L24
- Kellermann, K. I., Lister, M. L., Homan, D. C., Vermeulen R. C., Cohen, M. H., Ros, E., Kadler, M., Zensus, J. A. & Kovalev, Y. Y. 2004, *ApJ*, 609, 539
- Knuettel, S., Gabuzda, D. C. & O’Sullivan, S. P. 2017, *Galaxies*, 5, 61
- Lico, R., Gomez, J. L., Asada, K. & Fuentes, A. 2017, *Galaxies*, 5, 57
- Lister, M. L. & Homan, D. C. 2005, *AJ*, 130, 1389
- Lyutikov, M., Pariev, V. I. & Gabuzda, D. C. 2005, *MNRAS*, 360, 869
- Mahmud, M., Coughlan, C.P., Murphy, E., Gabuzda, D. C. & Hallahan, D. R. 2013, *MNRAS*, 431, 695
- Murphy, E., Cawthorne, T. V. & Gabuzda, D. C. 2013, *MNRAS*, 430, 1504
- Pushkarev, A. B., Gabuzda, D. C., Vetukhnovskaya, Yu. N. & Yakimov, V. E. 2005, *MNRAS*, 356, 859
- Singh, C. B., Mizuno, Y. & de Gouveia Dal Pino, E. M. 2016, *ApJ*, 824, 48
- Striani, E., Mignone, A., Vaidya, B., Bodo, G. & Ferrari, A. 2016, *MNRAS*, 462, 2970